

# Brain aging and garbage cleaning

## Modelling the role of sleep, glymphatic system and microglia senescence in the propagation of inflammaging

Susanna Gordleeva · Oleg Kanakov · Mikhail Ivanchenko · Alexey Zaikin and  
Claudio Franceschi

Received: date / Accepted: date

**Abstract** Brain aging is a complex process involving many functions of our body and described by the interplay of a sleep pattern and changes in the metabolic waste concentration regulated by the microglia function and the glymphatic system. We review the existing modelling approaches to this topic and derive a novel mathematical model to describe the crosstalk between these components within the conceptual framework of inflammaging. Analysis of the model gives insight into the dynamics of garbage concentration and linked microglial senescence process resulting from a normal or disrupted sleep pattern, hence, explaining an underlying mechanism behind healthy or unhealthy brain aging. The model incorporates accumulation and elimination of garbage, induction of glial activation by garbage, and glial senescence

by over-activation, as well as the production of pro-inflammatory molecules by their senescence-associated secretory phenotype (SASP). Assuming that insufficient sleep leads to the increase of garbage concentration and promotes senescence, the model predicts that if the accumulation of senescent glia overcomes an inflammaging threshold, further progression of senescence becomes unstoppable even if a normal sleep pattern is restored. Inverting this process by "rejuvenating the brain" is only possible via a reset of concentration of senescent glia below this threshold. Our model approach enables analysis of space-time dynamics of senescence, and in this way, we show that heterogeneous patterns of inflammation will accelerate the propagation of senescence profile through a network, confirming a negative effect of heterogeneity.

---

S. Gordleeva  
Laboratory of Systems Medicine of Healthy Aging, Lobachevsky University, Nizhny Novgorod, Russia  
Tel.: +7-987-7540864  
E-mail: gordleeva@neuro.nnov.ru

O. Kanakov  
Laboratory of Systems Medicine of Healthy Aging, Lobachevsky University, Nizhny Novgorod, Russia

M. Ivanchenko  
Laboratory of Systems Medicine of Healthy Aging, Lobachevsky University, Nizhny Novgorod, Russia

A. Zaikin  
Institute for Women's Health and Department of Mathematics, University College London, London, United Kingdom;  
Laboratory of Systems Medicine of Healthy Aging, Lobachevsky University, Nizhny Novgorod, Russia;  
Department of Paediatrics and Paediatric Infectious Diseases, Sechenov First Moscow State Medical University (Sechenov University), Moscow, Russia

C. Franceschi  
Laboratory of Systems Medicine of Healthy Aging, Lobachevsky University, Nizhny Novgorod, Russia;  
Department of Experimental Pathology, University of Bologna, Bologna, Italy

**Keywords** Inflammaging · Aging · Waste solutes · Glymphatic System · Sleep · Microglia · Cell · Senescence

### 1 Introduction

Rejuvenation and finding the youth elixir has always been one of the most treasured dreams of mankind. However, to understand how to achieve such a goal or at least to increase longevity one should first understand the basic molecular and cellular mechanisms underlying the aging process. We know that aging is a very complex process, which can be envisaged as a super-network of simultaneously occurring processes [1,2] linked in a very intricate way and involving almost all the key functions of our body such as sleep. Thus, alterations in sleep quantity and quality can be directly associated with aging [3], and sleep disturbances are an important risk factor for the development of a variety of age-related diseases including neurodegenerative disorders [3,4], even though the neurobiological mechanisms underpinning the age-related sleep disorders remain unclear. Re-

cent studies of the glymphatic system provide a new understanding of the role of sleep in waste clearance in the brain. The glymphatic (glial-lymphatic) system is a recently discovered glial-dependent macroscopic waste clearance pathway for the central nervous system (CNS).

The glymphatic system functions mainly during sleep [5,6] and facilitates the metabolite clearance in the CNS through the flow of interstitial and cerebrospinal fluid via perivascular pathways [7]. The unique system of perivascular tunnels is formed by astroglial cells and specifically by the aquaporin-4 water channels expressed in astrocytic endfeet [7,8,6]. Recent studies showed that the glymphatic system also clears neurotoxic protein aggregates (e.g., amyloid-beta) that contribute to the development of neurodegenerative diseases including Alzheimer's disease [9–11]. Glymphatic clearance was reduced by 40% in aged mice relative to young ones [9] suggesting that the glymphatic pathway deteriorates with age, and thus favoring the accumulation of neurotoxic proteins and the development of neurodegenerative disorders.

The glymphatic system is not the only clearance system in the CNS [11]. The removal of neurotoxic proteins from the brain can also occur via transport across the blood-brain barrier [12], degradation by enzymes expressed in astrocytes [13], or cellular uptake into neurons and glia [14,15]. Accumulation of proteins in the extracellular space induces the activation of the immune effectors of the CNS — microglia and astrocytes [16], which perform the phagocytosis of toxic proteins and at the same time produce neurotoxic inflammatory cytokines.

The scientific interest in the role of microglia and astrocytes in aging and disease is growing at an accelerating rate. Microglia, the resident immune cells of the CNS, have key physiological roles in brain development and CNS homeostasis, including programmed cell death and clearance of neuronal debris after cell death and injury, and synaptic pruning [17–19]. Any disturbance of brain homeostasis, including infection or inflammation, results in microglia activation. Rodent and human studies show that normal aging chronically changes microglial phenotype, consistent with a pro-inflammatory response, even in the absence of pathological stimuli [18]. Aged microglia have higher expression of pro-inflammatory genes, increased production of pro-inflammatory cytokines, and reactive oxygen species (ROS), while anti-inflammatory cytokines and microglial activation inhibitory factors are down-regulated [20]. Normal aging also decreases the uptake of amyloid-beta by microglia [21]. Recently, it was found that activated microglia is responsible for the induction of A1-like reactive astrocytes during normal CNS aging [22]. Such phenotype of neuroinflammatory reactive astrocytes is characterized by the loss of the capability to carry out their normal functions and the release of a toxic factor that kills neurons and oligodendrocytes. The aging-

induced upregulation of reactive genes by astrocytes could contribute to the cognitive decline in vulnerable brain regions in normal aging. Studies in humans and rodents found that sleep deprivation increases peripheral markers of inflammation [23–25]. Besides, it was recently shown that acute and chronic sleep loss promotes the phagocytosis of astrocytes of heavily used and strong synaptic elements in response to the increased neuronal activity, which occurs during extended wakefulness. Interestingly, chronic sleep loss induces microglial activation and enhanced phagocytosis without signs of neuroinflammation [26]. Therefore, reduced work of the glymphatic system during extended sleep disruption may lead to a state of sustained microglia activation. Thus, chronic sleep disturbance and persistent microglial activation, even at a low level (microglial priming), can predispose the brain to pathological states [27,28].

Carroll and colleagues [29] showed that partial sleep deprivation activates the senescence-associated secretory phenotype (SASP) and promotes cellular senescence in older adult humans. Also, recently it was demonstrated that normal aging increases the expression of senescence markers within the microglia population and more widely in the cerebral cortex [30]. These data complement numerous recent studies showing that other cell types in the brain, including neurons, astrocytes, and neuronal progenitors, display typical characteristics of cellular senescence in the normal aged brain [31,32]. Senescent cells are characterized by permanent cell cycle arrest, increased release of inflammatory factors, and production of a distinct SASP [33]. Senescent cells accumulate with age and at sites of age-related diseases throughout the body, where they actively promote tissue deterioration. Furthermore, studies have demonstrated that cellular senescence is transmissible and can spread to neighboring cells via secretory molecules [34,35]. Although relatively low in number, senescent macrophages are believed to be significant contributors to inflammaging, a phenomenon characterized by an age-related chronic, sterile, low-grade inflammation [36–39].

In aging, we observe a complex interaction between several players/stressors, i.e. aging, sleep disturbance, cell senescence, inflammaging, and correlated diseases, such as Alzheimer's disease or depression (Figure 1). Sleep disturbance is prospectively associated with age-related morbidity and mortality, possibly by fueling inflammaging. Inflammation, glia, and sleep seem to be linked in a complex system of processes. The recently discovered control of brain inflammation by gut molecules [41] is also involved in triggering and disturbing these processes by propagatory exosomes.

This raises the question: how cell senescence, microbiota dysbiosis, sleep disturbance, and systemic inflammaging interact to drive the brain into aging? Here, we propose a novel model to understand the underlying mechanisms behind all these interconnections. In order to provide a more

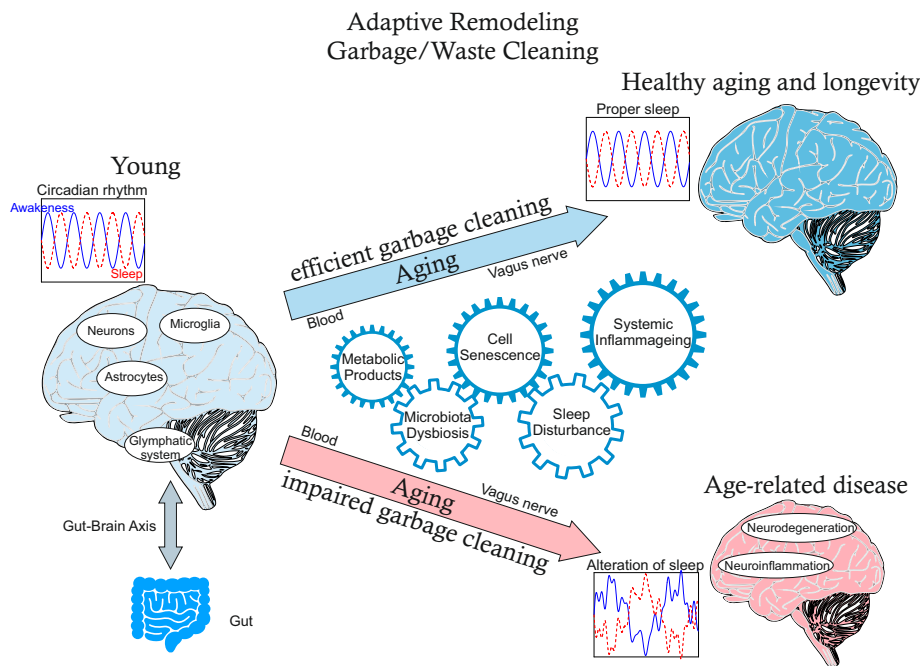


**Fig. 1** A brain is a complex super-network, or network of neurons, astrocytes, and microglia networks, interacting in a very complex way. An interplay of impaired metabolic products, cell senescence, systemic inflammaging, sleep disturbance, and microbiota dysbiosis drives this complex brain network of networks towards healthy or accelerated aging. A young brain has enough capacities to compensate if something goes wrong, but with aging, imbalance may increase and, triggered by sleep disturbances, wrong gut microbiota or malfunctioned garbage [40] cleaning, induce inflammation propagation through the brain network resulting in aging and age-related diseases (red bottom picture) instead of healthy aging and longevity (blue top).

comprehensive review of the full model, we will also discuss the mathematical models that have been recently developed to describe these ingredients separately (reduced formulation of the full model).

## 2 Mathematical models of aging mechanisms

The complexity of the aging process has motivated scholars to use mathematical modelling to synthesize knowledge discovery, generate hypotheses, and propose new experiments. Let us review several existing modelling approaches to aging, but first, it is important to emphasize that our approach is very different from population aging and mortality models, like the Gompertz-Makeham law [42]. For many years, scientists tried to develop a mathematical model of aging processes resembling the Brown [43], Penna [44], or Heumann-Hoetzel model [45], including different network models [46–48], describing mortality rate as a function of age.

In parallel, many extensive studies included the programmed aging theory [49], the rate of life theory [50,51], the theory of mutation accumulation [52,53], the oxidative damage theory [54,55], the theory of antagonistic pleiotropy [56], the threshold theory [57,58], the disposable soma theory [59], the mitochondrial and thermodynamic theories of aging [60], and, finally, the telomere and the redosome theory

of aging [61]. The latter approach was also used to introduce a mathematical expression for average life-span obtained for different telomere shortening strategies [62].

Mc Auley and Mooney recently reviewed the mathematical modelling methods of metabolic regulation in aging [63]. They discussed the main modelling frameworks, mostly based on computational models to describe separately the molecular mechanisms of aging [64]. These approaches suggested the models taking into account the DNA damage and repair [65], telomere shortening [66–68], loss of protein homeostasis [69], upregulation of molecular chaperones [70], protein degradation pathways [71,72], crosstalk between autophagy and apoptotic pathways subject to stress [73], protein aggregation [74–78], mitochondrial damage and ROS [79], mitochondrial dynamics [80], dysregulation of cellular signaling [81,82] and its influence on cellular senescence [83]. Among all the signal pathways, the nuclear factor- $\kappa$ B (NF- $\kappa$ B) plays the most important role affecting immunity, inflammation, cell differentiation, and apoptosis, all of which are activated by a range of stimuli, including infection, ROS and DNA damage [84,85]. There are a large number of models representing different aspects of NF- $\kappa$ B signaling, see [86,87] and refs therein. Another important role is played by cytokines, which are critical in the regulation of inflammatory responses, changing the level and effect of cytokines, as modelled in [88].

There is growing evidence suggesting the correlation between DNA methylation status and biological aging clock. Recently, several models have been used to mechanistically represent DNA methylation. These models could potentially be adapted to focus on crosstalk between DNA methylation and other elements of cellular aging [89], including age-related changes in DNA methylation within stem cells [90]. Another breakthrough was the discovery that microRNAs (miRNAs) – evolutionarily conserved post-transcriptional non-coding gene regulators – regulate the lifespan of nematodes *C. elegans* [91]. Thus, modelling has helped to identify feedback and feed-forward loops in miRNA-mediated networks and has revealed interactions among miRNAs during the regulation of genes [92]. A decline in tissue regeneration is another important factor in cellular aging resulting from a decline in stem cell function [93,94]. Przybilla et al. [90] examined the role of age-related DNA methylation changes, and Duscher et al. [95] modelled the effect of aging on dynamics of mesenchymal stem cells population, showing that an age-related depletion in progenitor cells impairs the formation of new blood vessels.

The majority of the above-mentioned studies focus on a particular molecular mechanism of aging; and the way they are designed makes them difficult to modify or integrate into other studies. Therefore, it is difficult to combine them and study a unified model that describes several aging processes at once. The current understanding of biological aging as a complex process involving the interplay of many mechanisms – from molecular to physiological – requires a more integrative modeling approach. For example, an interesting model has been proposed in [96] describing an interconnected multilayer system applied to study how amyloid-beta levels change within the brain parenchyma and vasculature, incorporating the role of the glymphatic system. This model based on the mass conservation equations shows the importance of vessel stiffness and heart rate in maintaining the proper level of clearance of amyloid-beta from the brain to avoid neuro-pathologies. There is an extensive literature devoted to modeling the circadian clock [97], or the interaction between a circadian and cell cycle gene-protein regulatory networks [98]. However, there has been no mathematical description of how sleep and inflammation are linked to age-related diseases [99], how sleep parameters are linked to inflammation [25], how the sleep-immune crosstalk functions [100], and how waste clearance is linked to circadian clocks and sleep [101]. Describing such a complex interaction requires a more detailed study of sleep loss effect on promoted astrocytic phagocytosis and microglial activation in the cerebral cortex [26] with particular focus on the role of the glymphatic pathway in this scenario and in neurological disorders [102].

In this paper, we are trying to fill this gap and to understand the contribution of the interplay of sleep quality,

dynamics of waste concentration, microglial activation, age-related impairment of clearance systems, and cellular senescence in the CNS aging using a mathematical modelling approach.

### 3 Model of the interplay between sleep, immune and waste clearance in inflammaging

#### 3.1 Model architecture

The model we propose describes the interaction between healthy and senescent glial cells, waste, and SASP molecules and shows how inflammaging propagation can appear in a certain area of a human brain. The model follows the approach of chemical kinetics to describe the flow and transformations of the involved “species” (molecules, cells) within an elementary volume of brain tissue. The general architecture of the model along with the dynamical variables and corresponding kinetic equations are shown in Figure 2. To make the model clearer for understanding, we will put the basic characteristics of the model and their components in bold font.

**The concentration of waste or “garbage”** (cellular and molecular garbage: cell debris, resulting from cell death, misplaced or altered or oxidized molecules, gut microbiota products, internal exosome, etc.) [40] **is described by variable  $R$** . Garbage is produced as a byproduct of neuronal activity and eliminated through two mechanisms: uptake by astrocytes and microglia and via the astrocyte-dependent glymphatic pathway. These fluxes of garbage are shown with blue arrows in Figure 2. The model takes into account that the rate of garbage uptake by glial cells depends on the state thereof, which can be active, leading to fast cleaning, and normal/quiet state associated with slow cleaning. The activation of healthy glial cells is assumed to be determined by garbage concentration. The activity of neurons and the glymphatic system (both of which affect the balance of garbage concentration in the brain) exhibit time variability locked to the circadian rhythm, as indicated by black arrows. Following the experimental findings [5,6] we consider that **the glymphatic system is activated during sleep**. The gradual transition of glial cells from normal to senescent state (as indicated by the magenta arrow) is assumed to be induced by glial overactivation promoted by garbage accumulation, and also by SASP molecules (shown with a black arrow). **The fractions of the population of normally functioning glial cells and senescent glial cells are denoted as  $G$  and  $G_S = 1 - G$ , respectively**. Senescent cells produce **pro-inflammatory SASP molecules**, which are shown in red in the scheme and are **represented in the model by the concentration variable  $\tilde{S}$** . The model accounts for the diffusion of SASP through the tissue. A detailed mathematical description of the model is given in the Appendix section A.

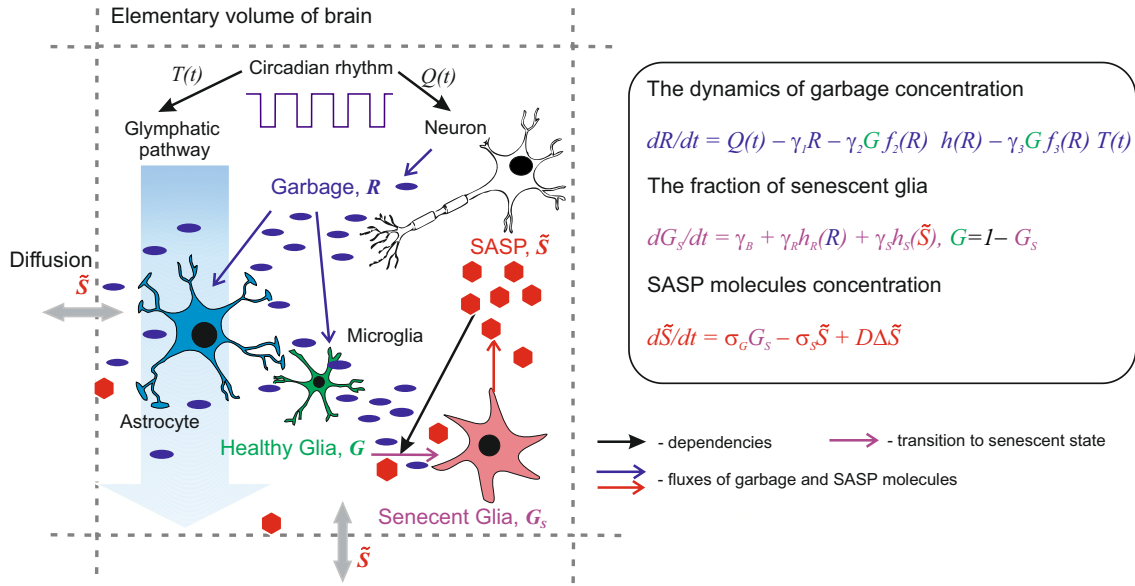


**Fig. 2** Schematics of the model: garbage is accumulated during neuronal activity and cleared by astrocytes (through the glymphatic pathway) and by microglia; neuronal activity and glymphatic system depend on the circadian rhythm; glial cells gradually transition from normal to senescent state; senescent cells produce pro-inflammatory SASP molecules; cell transition to senescence is potentiated by garbage and by SASP. Mathematical notations are detailed in the Appendix section A.

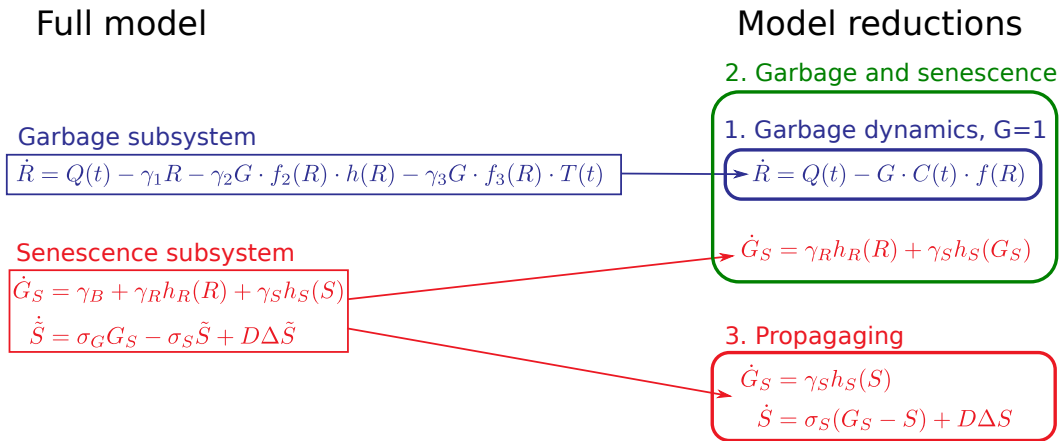


**Fig. 3** Model reductions: 1 — dynamics of garbage taken alone; 2 — joint dynamics of garbage and senescence without space-time effects; 3 — SASP-mediated self-propagation of senescence through the tissue (“propagating”). The reductions are derived and analyzed in the Appendix section B, and notations are summarized in Table 2.

### 3.2 Reduced formulations of the model

Our main goal is to show how the proposed model brings together the current conceptions of the roles of sleep, garbage accumulation, cell senescence, and propagation of inflammation in brain aging. More specifically, we focus on the following three aims: first, we fit the model parameters to reproduce the expected dependence of garbage accumulation on the sufficiency of sleep; second, we demonstrate the adequacy of the model in reproducing the expected impact of sleep deficiency and garbaging on glial senescence in the brain; third, we obtain propagating solutions in an inhomogeneous medium to describe the propagation of cell senescence

(**propagation of inflammaging or “propagating”** [40]). Here, we employ **three distinct reduced formulations of the model** based on specific simplifying assumptions. In this subsection, we outline these simplifications and the resulting reductions of the full model. Our main results, as outlined in Table 1, along with the respective subsections of the Appendix, are associated with the mentioned steps and are based on the respective reduced formulations of the model.

The investigated model can be seen as **two interacting subsystems**, as shown in the left part of Figure 3. **The first subsystem** (shown in blue) **describes the dynamics of garbage concentration**, which is determined by the balance

of garbage production by neurons, and its removal by microglia and astrocytes. Sleep and wakefulness are accounted for by explicit time dependence of both **production and removal rates (functions  $Q(t)$  and  $T(t)$  in the model)**. Additionally, the garbage removal rate depends on the garbage concentration itself. This dependence can generally account for glial cell activation and the saturation of the garbage elimination system. For the sake of analysis and due to the lack of experimental data to support any further detail of the model, we assume that **the time and concentration dependence of the garbage removal rate factorizes into a product of two functions  $C(t)$  and  $f(R)$ , which separately describe both dependencies**. This simplification of the garbage subsystem is shown in Figure 3 to the right of the blue arrow tip.

Furthermore, **the garbage removal rate is proportional to the quantity of non-senescent glia  $G$** . Generally speaking, this binds the dynamics of garbage to that of glial senescence. Following a recent experimental study [30] **we assume that the percentage of senescent glia is relatively small, which allows us to neglect the factor of glial senescence by taking  $G = 1$  in the dynamics of garbage**. Within this approximation, the garbage dynamics decouples from other variables of the model and can be studied separately. This (garbage only) reduction of the model consists of a single equation within the blue outline numbered as 1 in the right-hand part of Figure 3. This reduced model is derived and used in the Appendix subsection B.1 to fit the model parameters and to study the dependence of garbage dynamics on sleep duration.

The second subsystem (further referred to as the **“senescence subsystem”** and shown in red in Figure 3) describes **the irreversible transition of glial cells to the senescent state**. Generally, three pathways of this transition are considered, which correspond to the three summands in the full dynamical equation for  $G_S$ : first, **spontaneous transition with constant rate**, which is not dependent on any other variables of the model; second, **garbage-activated transition via glial overactivation**, which is triggered by garbage concentration exceeding a specific threshold; third, **SASP-mediated self-induction of cell senescence**, which is conditioned by SASP originating from senescent cells, which kicks in when the SASP concentration exceeds a respective threshold. We abstract from spontaneous senescence (which can be superimposed on top of our model dynamics if needed) by dropping  $\gamma_B$  and focus on garbage-induced and self-induced (SASP-mediated) senescence. As long as we neglect the dependence of garbage dynamics upon glial cells senescence (see above), the influence of the garbage subsystem upon the senescence subsystem is unidirectional.

The senescence subsystem contains **two dynamic variables**, which are **the quantity of senescent cells  $G_S$  and the concentration of SASP  $\tilde{S}$** . To cut down the number of inde-

pendent parameters of the model, we use a rescaled variable  $S$  for SASP concentration, as described in the Appendix subsection B.2. We consider two simplified versions of these full equations; these simplifications are pointed at by two red arrows in Figure 3. The first simplification starts from **dropping the diffusion of SASP** (thus abstracting from any space-time effects and considering the brain as a whole), which is followed by a quasi-steady-state approximation for the SASP concentration (assuming that it equilibrates much faster than the time scale of glial senescence). Within this simplification, the senescence subsystem reduces to a single ordinary differential equation for the quantity of senescent cells  $G_S$ . This equation combined with the garbage subsystem constitutes the second reduction of the model which is shown in the green outline numbered 2 in the right-hand part of Figure 3. This reduced model is derived and used in the Appendix subsection B.3 to study the impact of sleep deficiency and garbaging on glial senescence.

The other simplification of the senescence subsystem takes into account **SASP diffusion**, but abstracts from garbage-induced senescence, **focusing on SASP-mediated self-induction senescence** and on its propagation through the tissue due to the diffusion of SASP (“propagating”). Within this simplification, **garbage is viewed only as the initial cause of senescence in a localized spot in the tissue**. After propagating sets in, it becomes self-sustained and not dependent on further induction by garbage. This results in the third reduction of the model, which is shown in the red outline numbered 3 in the right-hand part of Figure 3 and used in the Appendix subsection B.4 to study the propagating phenomenon.

## 4 Results

The main results and predictions of the models we applied are summarized in Table 1, while their detailed mathematical description is reported in the Appendix.

## 5 Discussion

We have systematized currently available data on the mechanisms of brain aging and inflammation. In particular, these data include the causal chain from sleep deficiency and/or glial age-related decline in garbage cleaning to garbage accumulation (referred to as “garbaging” [40]), and then to senescence of glial cells and their accumulation as a consequence of garbage overactivation [36], and finally to self-induction of the glial senescence process mediated by the SASP molecules, which results in the perpetuation of inflammation [37]. We show that these causal connections boil down to a mathematical model describing the dynamics of key quantities characterizing brain inflammatory ag-

Increasing level of the model complexity	Predictions of the model
Garbage dynamics: daily variability of garbage production and elimination rates	A reduced formulation of the model describes how different wake/sleep patterns affect garbage concentration. The model shows that sleep deficiency (e.g. 5 hours of sleep in comparison to 8 hours of normal sleep) leads to the accumulation of garbage.
Joint local dynamics of garbage and cell senescence, coordinated by the production of SASP molecules	Insufficient sleep lead to an increase of garbage concentration due to promoted cell senescence and to the production of SASP pro-inflammatory molecules. SASP molecules in turn transfer senescence to neighboring glial cells. The model predicts that if accumulation of the senescent glia overcomes the inflammaging threshold, further progression of cell senescence becomes self-sustained, even after a normal sleep pattern is restored. The model shows that the replacement of senescent cells by healthy cells may potentially lead to “brain rejuvenation”, by promoting the slowdown of inflammaging.
Space-time dynamics of garbage and senescence taking into account the diffusion of SASP molecules	This full model enables the description of propagating, i.e. the propagation of cell senescence in the brain, and predicts that the spatial inhomogeneity of senescent cells favors the propagation of inflammaging.

**Table 1** Model results and predictions

ing, which include the quantities of garbage, senescent glial cells, and pro-inflammatory SASP. Thus, the model incorporates the description of the main factors involved in the process of brain inflammatory aging assuming: i) the main role of sleep in cleaning the brain of the toxic substances produced during wakefulness, here collectively called “garbage”; ii) sleep disorders, such as short sleep duration, disrupt the physiological circadian fluctuation of brain garbage production and cleaning. Sleep shortage increases the production of molecular garbage by extending wakefulness (i.e. the period of neuronal activity when the production of garbage is higher) and reducing the period devoted to garbage cleaning (which is maximal during sleep), operated by garbage-driven astrocyte/glia activation concomitant with the opening of the glymphatic system. Thus, the model reproduces expected phenomena like garbage upsurges associated with episodes of sleep deficiency, but also the lifelong accumulation of senescent glia acquired during supra-threshold upsurges of garbage and self-sustained pro-inflammatory SASP-mediated development of glial senescence after the quantity of senescent cells accumulates past a corresponding threshold.

Even though all the assumptions of the model are supported by a variety of experimental data (see Introduction), there is an urgent need for much more detailed data for better quantification of these phenomena and their interrelations. These considerations are particularly important for a key phenomenon predicted by the model, such as the induction of glial senescence by an unmatched excess of garbage overproduction and glial overactivation. The model also predicts that: i) the production of pro-inflammatory SASP molecules by senescent glial cells and their diffusion will lead to self-sustained glial senescence that in turn will propagate inflammaging throughout the brain [40]; ii) the inhomogeneous cell senescence background may lead to faster propagation than it would be in case of homogeneous senescence with

the same average. New experimental data are expected to test and verify this model prediction.

Despite the fact that it goes beyond the scope of this paper, the model allows the inclusion of the mechanism describing how gut molecules control brain inflammation [41], and how microbiota can program neuronal function by controlling intestinal physiology [103]. Additional experimental data on this topic are highly welcome to properly implement the possible extension of the model to the role of the gut microbiota in brain inflammaging.

In conclusion, the model presented here puts together basic phenomena involved in brain aging that are usually treated separately, focusing on the mechanisms underpinning a fundamental aspect of the aging process such as chronic inflammation/inflammaging. It is important to stress that a basic characteristic of the model is to link brain inflammatory aging to what is assumed to be a major physiological role of sleep, i.e. to clearing the brain from the toxic substances which accumulate during wakefulness. This assumption fits with data suggesting that a major characteristic of centenarians (assumed as the best model of healthy aging and longevity in humans) is optimal sleep duration and the maintenance of circadian rhythms, including sleep [104] and has far-reaching consequences regarding the role of sleep disorders and brain inflammation in increasing the risk of a variety of chronic age-related diseases [105,106]. Finally, the model predicts that it is possible to rejuvenate an aging brain by preventing the accumulation of senescent cells and the self-sustained pro-inflammatory SASP-mediated propagation of inflammation throughout the brain. This is a very interesting perspective owing to the number of emerging “senolytic” agents capable of targeting and clear senescent cells in different organs and tissues [107]. In animal models, the accumulation of senescent cells is associated with multiple chronic age-related diseases and accelerated aging phenotypes that can be prevented or de-

layed by decreasing senescent cells abundance [108]. Regarding the brain, as discussed throughout the present paper, senescent cells are present in the aging brain [31] and in the brain of Alzheimer's and Parkinson's disease models [109, 110]. Senescent cell markers were shown to be preferentially present within astrocytes in brain tissues of patients affected by Parkinson's disease, and paraquat was found to induce in mice astrocytic senescence and a SASP in vitro and in vivo, while senescent cell depletion protected against paraquat-induced neuropathology [111]. An interesting paper recently showed that in a mouse model of tau-dependent neurodegenerative disease, the clearance of senescent astrocytes and microglia prevented many neuropathological markers of the disease, including gliosis, neurofibrillary tangle deposition, degeneration of cortical and hippocampal neurons and preserved the cognitive functions [112]. Preliminary reports show that the senolytic approach is also effective in humans [113] but, as far as we know, no report has been published on senolytic therapy in patients affected by neurodegenerative diseases. However, it can be predicted that targeting senescent glial cells, i.e. astrocytes and microglia will represent a new therapeutic strategy in neurodegenerative diseases, and our model predicts that this approach will be capable of "rejuvenating" aged brain. New data on this hot topic are expected soon, and they will allow us to refine our model to better quantify the effect of the senolytic approach aimed at preventing the accumulation of senescent cells in the brain.

**Acknowledgements** We acknowledge support by the grant of the Ministry of Education and Science of the Russian Federation Agreement No. 074-02-2018-330(1). AZ thanks MRC grant MR/R02524X/1.

## A Model detalization

The changes in the concentration of garbage in a certain volume of brain are determined by the balance of its accumulation during neuronal activity on the one hand, and its degradation and clearance by microglial cells and astrocytes on the other. In space-time studies, we neglect the garbage diffusion, assuming it to be much slower than that of SASP molecules (see Eq. (6) below). The dynamics of garbage concentration is then described by the following equation:

$$\dot{R} = Q(t) - \gamma_1 R - \gamma_2 G \cdot f_2(R) \cdot h(R) - \gamma_3 G \cdot f_3(R) \cdot T(t), \quad (1)$$

where  $Q(t)$  denotes the (time-dependent) garbage production rate,  $\gamma_1$  is the rate of spontaneous degradation of garbage, and the two remaining terms describe two mechanisms of active garbage elimination: uptake by astrocytes and microglia (term with  $\gamma_2$ ) and the effect of glymphatic system (term with  $\gamma_3$ ).

The rate of garbage uptake by the glial cells depends on the state thereof, which can be active leading to fast cleaning, and normal quiet state associated with slow cleaning. The activation of the healthy glial cells is assumed to be determined by garbage concentration and is described by the function  $h(R)$ , which we assume to be a sigmoid function of the following form:

$$h(R) = x_0 - \frac{x_0 - 1}{1 + \exp\left(\frac{-(R-R_1)}{\eta_1}\right)}, \quad (2)$$

where  $x_0$  denotes the rate of waste clearance by non-activated microglia,  $R_1$  is the activation midpoint, and  $\eta_1$  is the inverse slope of the activation curve (see Figure 4(a)).

The glymphatic system is astrocyte-dependent and is activated during sleep. This daily variability is accounted for by the function  $T(t)$ .

The saturation of both garbage elimination systems is described by normalized nonlinear functions  $f_{2,3}(R)$ . Given no specific experimental data on either of them, we use a single function obtained from a kinetic description of garbage binding to glia:

$$f_{2,3}(R) = f_K(R) = \frac{R}{R_0 + R}, \quad (3)$$

where  $R_0$  is the saturation curve midpoint (which is the level of garbage concentration, where the elimination rate is half the maximum).

The conversion of glial cells to the senescent state is assumed to be induced by glial overactivation promoted by garbage accumulation, and also by SASP molecules, which are in turn constantly produced by the senescent cells. The progression of glial senescence is described by the following dynamical equation for the fraction of the senescent glia  $G_S$  (total quantity of glia assumed constant):

$$\dot{G}_S = \gamma_B + \gamma_R h_R(R) + \gamma_S h_S(S), \quad (4)$$

where  $\gamma_B$  is the background (always present) senescence rate,  $\gamma_R$  and  $\gamma_S$  control the rates of senescence induced by garbage and SASP,  $h_R(R)$  and  $h_S(S)$  are corresponding normalized activation functions, which are assumed to be sigmoid functions

$$h_R(R) = \frac{1}{1 + \exp\left(\frac{-(R-R_A)}{\eta_R}\right)}, \quad h_S(S) = \frac{1}{1 + \exp\left(\frac{-(S-S_A)}{\eta_S}\right)}, \quad (5)$$

where  $R_A$  and  $S_A$  are senescence activation midpoints for garbage and SASP,  $\eta_R$  and  $\eta_S$  determine the widths of the smoothed step transition (see Figure 4).

The changes of SASP molecules concentration  $\tilde{S}$  are determined by the balance of their production (by senescent astrocytes and microglia), natural degradation and diffusion, and are described by the equation

$$\dot{\tilde{S}} = \sigma_G G_S - \sigma_S \tilde{S} + D \Delta \tilde{S}, \quad (6)$$

where  $\sigma_G$  is the rate of SASP production by senescent cells,  $\sigma_S$  is SASP degradation rate,  $D$  is the diffusion coefficient, and  $\Delta$  is the Laplacian operator.

## B Model reductions

Here we derive and analyze the reduced formulations of the model, as described in the subsection 3.2. All notations are additionally summarized in Table 2.

### B.1 Dynamics of garbage concentration

Assuming the rate of spontaneous garbage degradation to be much smaller than that of active garbage cleaning by glial cells, we neglect the term with  $\gamma_1$  in Eq. (1), transforming the latter into

$$\dot{R} = Q(t) - G \cdot [\gamma_2 f_2(R) \cdot h(R) - \gamma_3 f_3(R) \cdot T(t)]. \quad (7)$$

The factor in square brackets here describes the dependence of garbage elimination rate on time  $t$  and concentration of garbage  $R$ . Generally speaking, it cannot be factorized into a product of separate functions of  $t$  and  $R$ . That said, and taking into account the absence of experimental data to quantify all the unknown functions within the bracketed



Notation	Meaning Value and/or expression	Justification
$f(R)$	Accounts for the dependence (saturation) of garbage elimination rate upon garbage concentration. In analysis: piecewise linear function $f_P(R)$ as defined in Eq. (9). In simulations: smoothed function $f_K(R)$ as in Eq. (3) unless stated otherwise (see details in the text). Function parameter: $R_0$ (characteristic concentration of garbage at which the garbage elimination system starts to saturate).	
$R_0$	1	We assume that $R_0$ is normalized to unity by scaling the measurement unit of $R$ .
$C(t)$	Accounts for the time dependence (daily variability locked to the sleep pattern) of garbage elimination rate. Takes on two fixed values: $C_s$ during sleep and $C_w$ during wakefulness; switches abruptly between these values.	
$C_s$	$= \tau_s^{-1} = 6$ (“healthy” condition) $= 5.7$ (“aged” condition: cut down by 5%)	An indicative estimate from (21) with a reasonable guess taken for the characteristic time scale of garbage elimination during sleep $\tau_s = 1/6$ (4 hours); the estimate is based on the piecewise linear saturation function $f(R) = f_P(R)$ as defined in Eq. (9), but as an indicative value applies regardless of the exact saturation function type.
$C_w$	$= C_s/2 = 3$ (“healthy” condition) $= 2.85$ (“aged” condition: cut down by 5%)	Assumption: the rate of garbage elimination during wakefulness is half of that during sleep, as justified in [5, 114].
$Q(t)$	Accounts for the time dependence (daily variability locked to the sleep pattern) of garbage production rate. Takes on two fixed values: $Q_s$ during sleep and $Q_w$ during wakefulness; switches abruptly between these values.	
$Q_s$	0	Assumption: negligible production of garbage during sleep.
$Q_w$	5	Obtained from (22) with a reasonable guess for the critical sleep duration $T_s^{\text{crit}} = 0.25$ (6 hours).
$\gamma_R, \gamma_S$	The rates of two pathways of cell transition to senescence: $\gamma_R$ — garbage-activated transition via glial overactivation; $\gamma_S$ — SASP-mediated self-induction of cell senescence. $10^{-4}$	Indicative estimate based on the assumption that the fraction of senescent cells $G_S$ gets an increment of 0.1 (equivalently, 10%) in 500 days when both activation by garbage and self-induction via SASP are present.
$h_R(R), h_S(S)$	Normalized activation functions which determine when the two pathways of cell transition to senescence come into play: $h_R(R)$ — garbage-activated transition via glial overactivation; $h_S(S)$ — SASP-mediated self-induction of cell senescence. In analysis: Heaviside step functions (23). In simulations: sigmoid functions (5). Function parameters: $R_A$ and $S_A$ (threshold values), $\eta_R$ and $\eta_S$ (widths of the step transitions).	
$R_A$	15	Fitted to comply with the indicative assumption that 20 days of sleep deficiency (5 hours sleep duration) or 7 days of complete sleep deprivation trigger garbage-induced senescence. This estimate is based on numerical simulations with the smooth saturation function $f(R) = f_K(R)$ as defined in Eq. (3).
$\eta_R$	$= R_A/15 = 1$	Indicative guess ( $\eta_R \ll R_A$ ).
$S_A$	0.1	$S_A$ is the critical value for the fraction of senescent cells $G_S$ . Namely, after $G_S$ rises above $S_A$ , senescence starts to self-activate via SASP production. The value of $S_A = 0.1$ estimates this critical fraction as 10%.
$\eta_S$	$= S_A/20 = 0.005$	Indicative guess ( $\eta_S \ll S_A$ ).
$\sigma_S$	Inverse characteristic time scale of SASP concentration equilibration: $\sigma_S = \tau_S^{-1}$ .	
$D$	SASP diffusion coefficient. 1	In the space-time simulations we assume that both constants are normalized to unity by a proper simultaneous scaling of time and space units.

Table 2 Model notations summary.

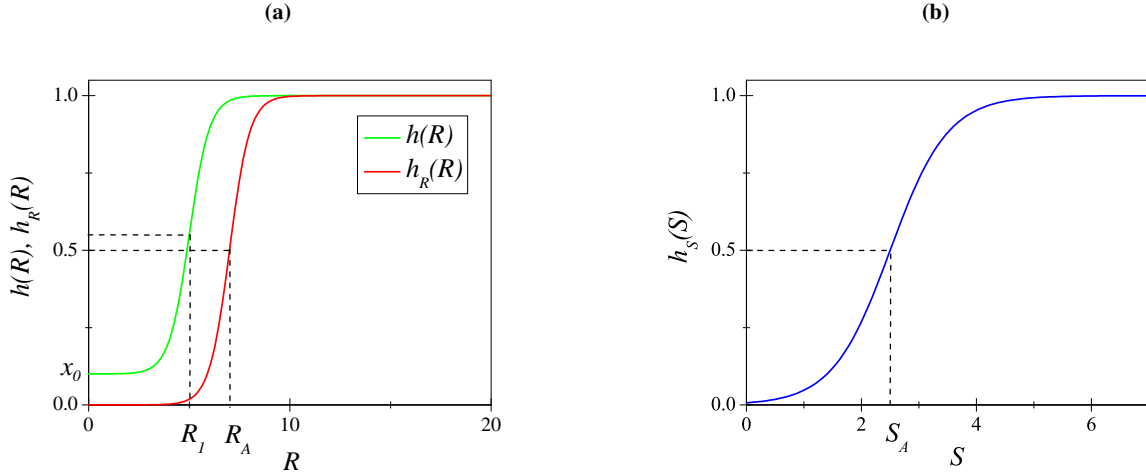


**Fig. 4** Model functions: (a) describes activation  $h(R)$  of healthy glial cells clearing garbage as a function of the garbage concentration  $R$ , whereas the function  $h_R(R)$  describes an increment of senescent cell proportion, when glial cells are overactivated as a result of garbage accumulation; (b) illustrates the function  $h_S(S)$  describing a transition between healthy and senescent cells in the course of interaction with SASP molecules.

expression, for the sake of model simplicity, we artificially impose the assumption of such factorization, which reduces the equation to the form

$$\dot{R} = Q(t) - G \cdot C(t) \cdot f(R), \quad (8)$$

where  $C(t)$  characterizes the time dependence of garbage elimination, and  $f(R)$  the concentration dependence. For the sake of analytical consideration, we use a simplified piece-wise linear saturation function

$$f(R) = f_P(R) = \max\{1, R/R_0\}, \quad (9)$$

and in numerical simulations also the smooth function  $f(R) = f_K(R)$  as defined in Eq. (3).

Following this approach, we essentially abstract from quantifying the effect of glial cells activation (given by the function  $h(R)$  in the full model (1)). If taken into account, glial activation would show up as a section with steeper dependence of garbage elimination rate upon garbage concentration somewhere below the saturation level (at  $R \lesssim R_0$ ). We argue that this would only have a quantitative impact, while our main qualitative results remain mainly determined by saturation effects, which we necessarily take into account. Therefore, we limit ourselves to a paradigmatic model in the form (8), considering further detalization currently unattainable due to the aforementioned lack of experimental data.

Hereafter we assume that  $R$  is measured in the units of  $R_0$ , which implies  $R_0 = 1$ .

For further simplification, we recall that the fraction of the senescent glia is typically a small value. A quantitative reference for the number or frequency of senescent microglia/ macrophages in the aged brain is currently lacking, due in part to the complexity of defining specific criteria for glial senescence in vivo. In a recent study, the percentage of senescent microglia ranged from 1% to 4% of the total population [30]. This is consistent with senescent cell numbers in other tissues and reflects a significant number of dysfunctional senescent cells. Indeed, very small numbers of transplanted senescent cells are enough to cause lasting physical dysfunction [115, 116]. Hence, we assume  $G = 1$  without significant impairment of model precision.

To account for daily variability of garbage production and elimination rates, we assume that  $Q(t)$  and  $C(t)$  take on different constant values during wakefulness and sleep, these values further respectively denoted as  $Q_w, C_w$  and  $Q_s, C_s$ .

Finally, the simplified version of (8) which we will analyze reads

$$\dot{R} = \begin{pmatrix} Q_w \\ Q_s \end{pmatrix} - \begin{pmatrix} C_w \\ C_s \end{pmatrix} \cdot f_P(R), \quad (10)$$

where the upper and the lower symbols correspond to wakefulness and sleep.

As soon as the piece-wise linear saturation function  $f_P(R)$  (9) is used, equation (10) implies accumulation or decay of garbage at a constant rate above the saturation threshold in  $R$

$$\dot{R} = Q - C, \quad \text{when } R > 1, \quad (11)$$

and reduces to a linear equation below the saturation threshold

$$\dot{R} = Q - CR, \quad \text{when } R \leq 1. \quad (12)$$

Natural assumptions are

$$Q_w > C_w, \quad (13)$$

otherwise, according to (12), a stationary concentration of garbage  $R_\infty = Q_w/C_w < 1$  would be attained even without sleep, thus rendering sleep unnecessary, and

$$Q_s < C_s, \quad (14)$$

otherwise elimination of garbage during sleep would be impossible.

We measure time in days and denote the duration of sleep as  $T_s$ , and that of wakefulness as  $T_w = 1 - T_s$ . We note that whenever

$$(Q_w - C_w)T_w > (C_s - Q_s)T_s, \quad (15)$$

equation (11) leads to infinite accumulation of garbage, thus there exists a critical sleep duration  $T_s^{\text{crit}}$  determined by

$$(Q_w - C_w)(1 - T_s^{\text{crit}}) = (C_s - Q_s)T_s^{\text{crit}}. \quad (16)$$

If  $T_s > T_s^{\text{crit}}$  (sufficient sleep), garbage concentration during sleep falls below the saturation level ( $R < 1$ ), and during wakefulness may or may not exceed the saturation level. Established dynamics of garbage concentration in this regime is shown in Figure 5(a). Here we use the values of parameters  $Q_w = 5, C_w = 3, Q_s = 0, C_s = 6$ , which are justified below, along with  $T_s = 1/3$  which corresponds to a sleep duration of 8 hours.

At the critical sleep duration  $T_s = T_s^{\text{crit}}$  garbage concentration  $R(t)$  in the stationary regime demonstrates a saw-like profile with minimum at the saturation threshold  $R = 1$  and with maximum

$$R_{\text{max}}^{\text{crit}} = C_s T_s^{\text{crit}} + 1. \quad (17)$$

Established dynamics of garbage concentration in the critical regime is shown in Figure 5(b) with the value  $R = R_{\max}^{\text{crit}}$  marked with a red dashed horizontal line. Here sleep duration is  $T_s = 1/4$  (equivalent to 6 hours), other parameters same as above.

If  $T_s < T_s^{\text{crit}}$  (insufficient sleep), then garbage concentration inevitably rises above the saturation level ( $R > 1$ ) and accumulates infinitely (while the deficiency of sleep is present) with average rate

$$\langle \dot{R} \rangle = (Q_w - C_w)T_w - (C_s - Q_s)T_s. \quad (18)$$

Dynamics of garbage accumulation in this regime is shown in Figure 5(c) with the average trend  $R(t) \sim \langle \dot{R} \rangle \cdot t$  shown with a red dashed line. Here sleep duration is  $T_s = 5/24$  (5 hours).

In order to fit the model parameters to reality, we start with the assumption that garbage production during sleep is negligible compared to that during wakefulness ( $Q_s \ll Q_w$ ), so further we let  $Q_s = 0$  for simplicity. The remaining model parameters  $Q_w$ ,  $C_w$ ,  $C_s$  can be quantified using the following considerations for a healthy human.

During sleep the dynamics of garbage in the unsaturated regime (when  $R < 1$ ) is described by the linear equation (12), which reduces to

$$\dot{R} = -C_s R, \quad (19)$$

and implies exponential decay of garbage concentration to zero

$$R(t) \sim e^{-t/\tau_s} \quad (20)$$

with characteristic time scale

$$\tau_s = \frac{1}{C_s}. \quad (21)$$

Then sleep periods greatly exceeding  $\tau_s$  (for definiteness,  $T_s > 2\tau_s$ ) are excessive in the sense that further sleeping does not improve garbage elimination significantly. Estimating this sufficient sleep duration as 8 hours, we get  $\tau_s$  equal to 4 hours, or in the units of days  $\tau_s \approx 1/6$ , which produces an estimate  $C_s \approx 6$ .

In order to estimate the two remaining parameters  $Q_w$  and  $C_w$ , we generally need two additional biologically relevant quantitative model outcomes to correlate with reality. For one of them, we use the critical sleep duration  $T_s^{\text{crit}}$ , for which from (16) we get

$$Q_w - C_w = \frac{C_s T_s^{\text{crit}}}{1 - T_s^{\text{crit}}}. \quad (22)$$

Estimating  $T_s^{\text{crit}} \approx 0.25$  (6 hours), and using the above estimate  $C_s \approx 6$ , we get  $Q_w - C_w \approx 2$ . Due to scarcity of quantitative experimental data on the dynamics of garbage concentration in the brain, we further employ the observation of [5, 114] that the rate of garbage elimination during sleep is roughly twice than that during wakefulness, which finally yields  $C_w \approx C_s/2 \approx 3$ ,  $Q_w \approx C_w + 2 \approx 5$ . This set of parameters was used to produce the profiles of  $R(t)$  in Figure 5 and is used hereinafter, unless stated otherwise.

When the piece-wise linear saturation function (9) in the model is replaced by a more realistic smooth function (3), with parameter values unchanged, the quantitative dynamics  $R(t)$  changes, but the qualitative behavior remains. This can be seen in Figure 6, where panel (a) corresponds to normal sleep duration (8 hours) and panel (b) shows the accumulation of garbage in case of sleep deficiency (5 hours of sleep). Remarkably, the expression for average trend (18) still produces a good estimate for garbage accumulation rate in the saturation regime (shown with the red dashed line in the figure).

## B.2 Dynamics of glial senescence

The sigmoid activation functions  $h_R(R)$  and  $h_S(S)$  (5) from dynamical equation for the fraction of senescent glia (4) for the sake of analysis can be written in the step form

$$h_R(R) = H(R - R_A), \quad h_S(S) = H(S - S_A), \quad (23)$$

where  $H(\cdot)$  is the Heaviside step function.

The balance equation for the unnormalized SASP concentration (6) allows for arbitrary rescaling of its variable of state, which allows to eliminate one of its parameters. We make such rescaling by introducing a normalized SASP concentration variable  $S$  according to

$$\tilde{S} = \frac{\sigma_G}{\sigma_S} S, \quad (24)$$

so that the unitary concentration  $S = 1$  is now defined as the (actually unattainable) stationary concentration of SASP, which would be achieved if all the glia were senescent ( $G_S = 1$ ). In this notation, the balance equation (6) transforms into

$$\dot{S} = \sigma_S(G_S - S) + D\Delta S, \quad (25)$$

where the parameter  $\sigma_S$  determines the characteristic time scale  $\tau_S$  of SASP concentration equilibration

$$\sigma_S = \frac{1}{\tau_S}. \quad (26)$$

## B.3 Local dynamics of garbage and senescence

To characterize the joint dynamics of glial senescence and SASP, we first consider their local dynamics, which implies  $D\Delta S = 0$  in (25). This corresponds to the absence of diffusion  $D = 0$ , or to the spatially uniform case with  $\Delta S = 0$ .

Assuming the time scale  $\tau_S$  of SASP dynamics to be much smaller (faster) than that of glial senescence, we can replace  $S$  in (4) by its quasi-steady-state approximation from (25), which is

$$S = G_S. \quad (27)$$

Additionally, in order to focus on garbage-induced senescence, we neglect the background (garbage-independent) senescence by taking  $\gamma_B = 0$ . This way equation (4) is transformed into

$$\dot{G}_S = \gamma_R h_R(R) + \gamma_S h_S(G_S). \quad (28)$$

Model (4) implies that the quantity of senescent glia never decreases. In the version (28) with step functions (23) taken for  $h_R(\cdot)$  and  $h_S(\cdot)$  senescence at best does not progress ( $G_S = \text{const}$ ) while  $R < R_A$  and  $G_S < S_A$ , and increases otherwise.

In other words, while senescence remains below its threshold ( $G_S < S_A$ ), the accumulation of senescent glial cells is conditioned by garbage and occurs only when the latter exceeds its respective threshold ( $R \geq R_A$ ).

As soon as senescence due to its course-of-life accumulation exceeds its threshold ( $G_S \geq S_A$ ), the right-hand side of (28) becomes positive regardless of the garbage level, which implies the monotonous accumulation of glial senescence due to a positive feedback via SASP even in the absence of further induction by garbage.

In this view,  $R = R_A$  is the ‘‘garbaging’’ threshold; its temporary overshoot by garbage concentration leads to an increase in the quantity of senescent glia, which however stabilizes (does not accumulate any more) once the garbage overshoot ends. The garbage increase, in turn, may be caused by a temporary deficiency or deprivation of sleep, as it follows from the garbage balance equation (8), according to the results

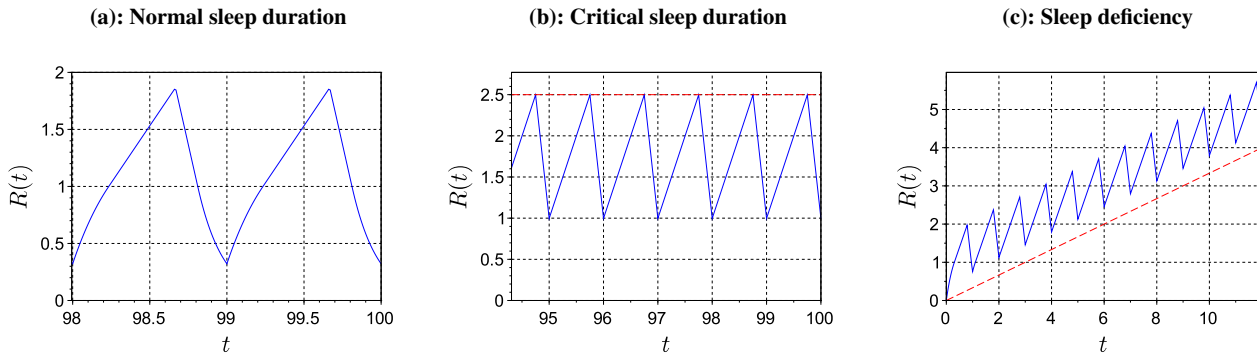


**Fig. 5** Dynamics of the garbage concentration  $R(t)$  in the simplified piece-wise linear model with  $Q_w = 5$ ,  $C_w = 3$ ,  $Q_s = 0$ ,  $C_s = 6$ : (a) — normal sleep (8 hours,  $T_s = 1/3$ ); (b) — critical regime of sleeping (6 hours,  $T_s = 1/4$ ), maximal value (17) shown with a red dashed horizontal line; (c) — insufficient sleep (5 hours,  $T_s = 5/24$ ), average trend (18) shown with a red dashed line.

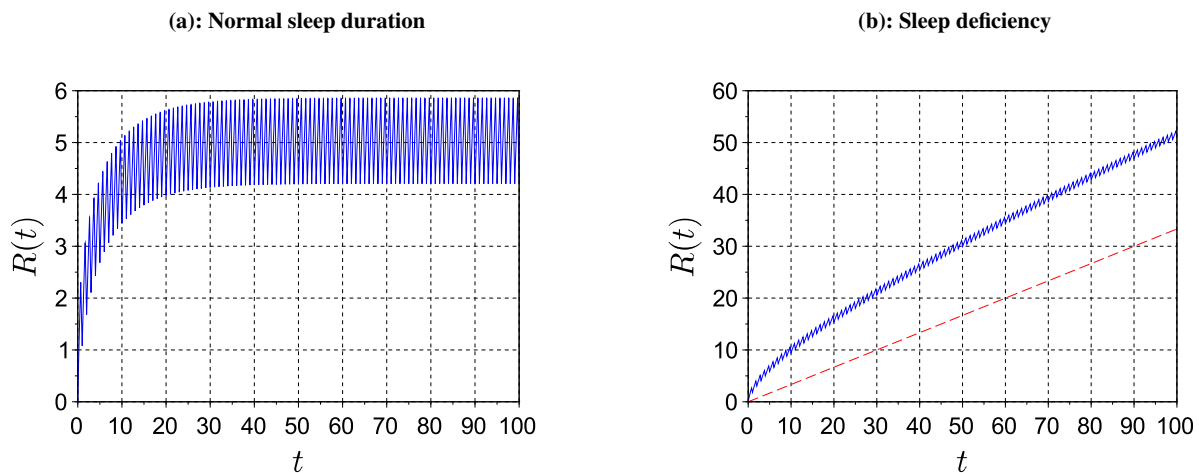


**Fig. 6** Dynamics of the garbage concentration  $R(t)$  in the model with smooth nonlinearity (6), parameters same as in Figure 5: (a) — normal sleep (8 hours,  $T_s = 1/3$ ); (b) — insufficient sleep (5 hours,  $T_s = 5/24$ ).

of the Section B.1. The height and the duration of a garbage concentration peak induced by a particular episode of sleep restriction depend increasingly upon the severity and the duration of sleep deficiency.

We illustrate this by simulating the joint dynamics of garbage concentration and glial senescence according to the equations (8) and (28) with smooth nonlinearities (3), (5). Parameters of garbage dynamics (8) are as in Section B.1, and for senescence dynamics (28), due to the lack of real data, we pick indicative quantities  $\gamma_R = \gamma_S = 10^{-4}$ , along with activation function parameters in (5)  $R_A = 15$ ,  $\eta_R = 1$ ,  $S_A = 0.1$ ,  $\eta_S = 0.005$ . In Figure 7(a) we show the simulation result on a time interval of 350 days. Most of the time the sleep duration is 8 hours ( $T_s = 1/3$ ), except for two episodes of sleep restriction ( $T_s = 5/24$  or 5 hours) lasting for 10 and 20 days, which correspond to the first two peaks in the garbage dynamics (the upper panel in 7(a)), and two episodes of complete sleep deprivation ( $T_s = 0$ ) lasting for 3 and 7 days, which correspond to the latter two peaks in the garbage dynamics. Indeed, we observe more pronounced garbage peaks as the duration of sleep deprivation or restriction is increased (the 2nd and the 4th peaks, as compared to the 1st and the 3rd). Expectedly, complete sleep deprivation (the 3rd and the 4th peaks) produces a steeper increase of garbage than sleep deficiency (the 1st and the 2nd peaks). We have chosen the garbaging threshold value  $R_A = 15$  so that only the more severe episodes of sleep restriction (20 days of sleep deficiency or 7 days of complete sleep deprivation) lead to the accumulation of glial senescence (the lower panel in Figure 7(a)).

To demonstrate the effect of an age-related decrease of garbage elimination rate upon the dynamics of garbage and glial senescence, we performed a similar simulation with garbage elimination rates  $C_s = 5.7$ ,  $C_w = 2.85$ , which are cut down by 5% compared to the previous simulation, all other conditions unchanged. The result is shown in Figure 7(b), showing higher garbage peaks and longer recovery times; moreover, all four episodes of sleep deficiency now produce glial senescence. The resultant increment of glial senescence over the same simulated time interval is now about 3 times greater than in the previous simulation (cf. Figure 7(a)).

In turn,  $G_S = S_A$  is the “inflammaging” threshold. When senescent glia accumulates beyond this threshold (due to accumulation of the above mentioned “garbaging” overshoots during the life course), further progression of senescence becomes monotonous due to self-induction via SASP and does not stop till the end of life. This is illustrated by the simulation result shown in Figure 7(c), where all conditions are the same as in Figure 7(b), except for starting from a higher value of the senescence variable  $G_S(t=0) = 0.085$  and extending the simulated time interval (the relevant part is up to  $t = 500$  days; the remaining part of the graph is discussed below). Here the senescence variable, once reached the inflammaging threshold  $S_A = 0.1$ , continues to grow even in the absence of garbaging peaks.

This feature of our model implies that inflammaging, once set in, never stops, even if the garbage elimination rate recovers to normal. More precisely, our model does not incorporate any mechanisms for inflammaging to stop. This follows from the assumptions that inflam-

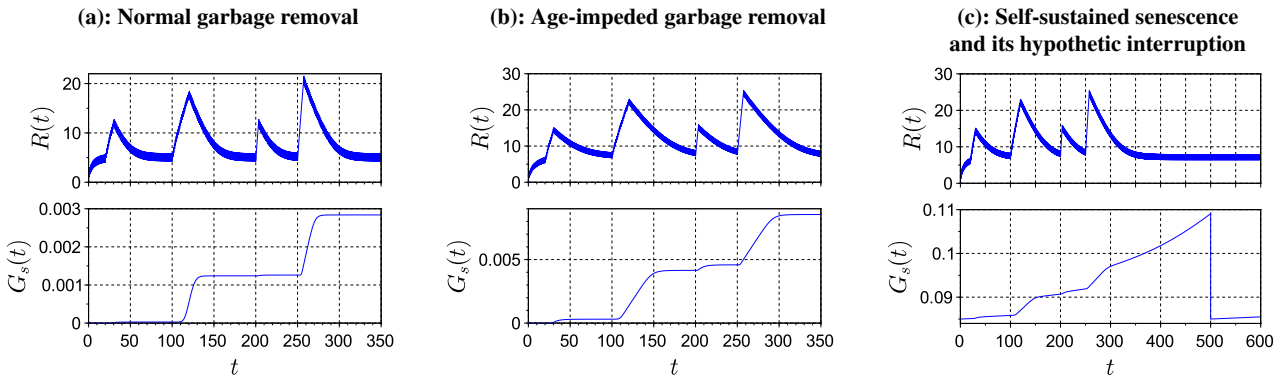


**Fig. 7** Simultaneous dynamics of the garbage concentration  $R(t)$  and the fraction of senescent cells  $G_S(t)$  in a variable sleep quality profile containing 2 periods of sleep deficiency and 2 periods of total sleep deprivation interleaved with normal sleep (see details in the text): (a) — garbage removal rates are at their normal values  $C_s = 6$ ,  $C_w = 3$ , as estimated in Section B.1; (b) — age-impeded garbage removal with  $C_s = 5.7$ ,  $C_w = 2.85$  (95% of the norm) leads to higher garbage peaks and greater accumulation of senescence; (c) — same age-impeded garbage removal on top of pre-existing age-related glial senescence  $G_S(t=0) = 0.085$  trigger the vicious circle of self-sustained SASP-mediated senescence; the hypothetical recovery of senescent glia breaks the vicious circle, as shown in panel (c) by resetting  $G_S$  at  $t = 500$  back to  $G_S(t = 500) = 0.085$ .

maging is driven by SASP, which in turn is produced by senescent cells, which remain in this state perpetually.

A hypothetical possibility to extinguish inflammaging would require a mechanism to eliminate senescent cells from the brain faster than they build up. Wong [117] and Clarke with colleagues [22] discuss the replacement of aged microglia with young microglia as the “rejuvenative” therapy. These microglial “replacements” may promote the removal of accumulated garbage, and the slowdown of the cellular senescence process, thereby improving cognitive function in aging. Prospects for the role of techniques for clearance of senescent macrophages in prolonging healthspan are actively discussed in the scientific community now [36]. We simulate such recovery of senescent glia by artificially resetting the variable  $G_S$  to a sub-inflammaging value  $G_S = 0.085$ , as shown in Figure 7(c) at  $t = 500$ . The concentration of senescent cells is now reset, self-induction and progression of senescence are stopped, and future behavior will again depend on whether sleep pattern and garbage elimination are normal or not.

#### B.4 Space-time dynamics of senescence (“propagating”)

The model in the form of ordinary differential equations considered in the Section B.3, where diffusion is dropped and quasi-steady-state approximation used to express SASP concentration, applies to the description of the dynamics of glial senescence in the brain taken as a whole, on large time scales up to the lifetime, or in local parts of the brain, while this local senescence does not propagate in space.

In order to describe the progression of senescence with spatial detalization, we revert to the full model consisting of the equations for glial senescence (4) and SASP balance (25) including the diffusion term. We focus on propagating solutions where glial senescence propagates itself through the tissue in the wake of diffusing SASP (a phenomenon referred to as propagation of inflammaging [40]). In this regard, we take an initial spatial profile of senescence at the onset of propagation as given, abstracting from its backstory and taking into account the only mechanism of senescence, namely that activated by SASP ( $\gamma_S \neq 0$ ), while assuming  $\gamma_B = 0$ ,  $\gamma_R = 0$  in (4). Although we recognize activation by garbage as the root cause initiating senescence, we consider it as part of the mentioned “backstory”, which is adequately described by local dynamics as in Section B.3, and hence we omit it in the model of inflammaging propagation.

Finally, we formulate the mathematical model as a system of simultaneous equations (4) and (25) with the assumptions above taken

into account:

$$\dot{S} = \sigma_S(G_S - S) + D\Delta S, \quad (29)$$

$$\dot{G}_S = \gamma_S h_S(S). \quad (30)$$

We simulate a two-dimensional system with spatial inhomogeneity introduced into the initial profile of the senescence variable  $G_S$ , as shown in panel (a) of Figure 8. To initiate inflammaging propagation, we place a patch with a sufficiently high senescence value in the center of the system. A typical snapshot of the senescence variable in color encoding taken at  $t = 25$  is presented in panel (b) of Figure 8.

We find that the spatial inhomogeneity of the initial senescence background may lead to faster propagation of the senescence front than it would be in case of homogeneous initial senescence with the same average. To quantify this statement, we calculate the ratio  $\varepsilon$  of the tissue volume with high level of senescence (where the condition  $G_S > S_A$  is fulfilled) to the total volume of the tissue. We compute  $\varepsilon$  over time in settings with homogeneous and inhomogeneous initial senescence backgrounds with the same average. The resulting plots are shown in Figure 9 confirming faster propagation of senescence in the inhomogeneous case.

This phenomenon can be explained by quicker propagation of the front in areas with greater initial senescence, which allows the inflammaging to cover quickly larger distance, even though leaving behind some non-inflamed “holes” in places where initial senescence was low. These holes eventually get taken over by the inflammaging propagation process without hindering the fast propagation of the foremost parts of the front.

#### Conflict of interest

The authors declare that they have no conflict of interest.

#### References

1. Brian K. Kennedy, Shelley L. Berger, Anne Brunet, Judith Campisi, Ana Maria Cuervo, Elissa S. Epel, Claudio Franceschi, Gordon J. Lithgow, Richard I. Morimoto, Jeffrey E. Pessin, Thomas A. Rando, Arlan Richardson, Eric E. Schadt, Tony Wyss-Coray, and Felipe Sierra. Geroscience: Linking aging to chronic disease. *Cell*, 159(4):709–713, November 2014.

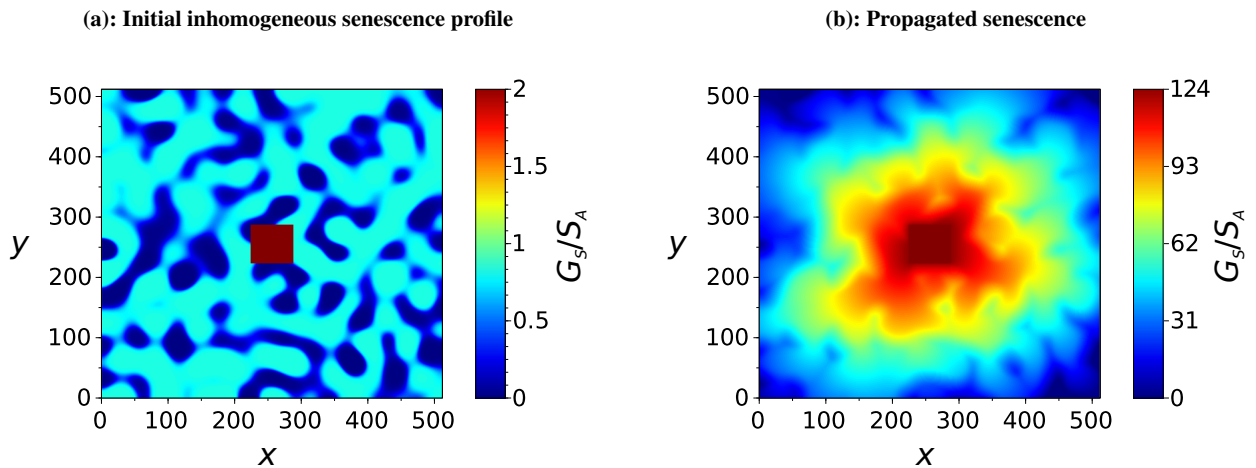


**Fig. 8** Simulating propagation of inflammaging over an inhomogeneous initial senescence profile in two-dimensional space. Level of senescence shown in color code: (a) — initial condition at  $t = 0$ ; (b) — snapshot at  $t = 25$ . Coordinates  $x$  and  $y$  are in arbitrary units.

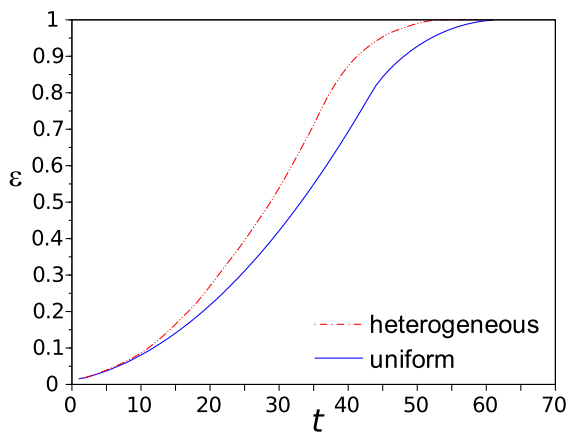


**Fig. 9** Propagation of inflammaging quantified by time evolution of the ratio  $\varepsilon$  of the tissue volume with high level of senescence ( $G_S > S_A$ ) to the total volume of the tissue in simulation runs with two different initial senescence profiles (uniform and inhomogeneous) with equal mean.

2. Harry J. Whitwell, Maria Giulia Bacalini, Oleg Blyuss, Shangbin Chen, Paolo Garagnani, Susan Yu Gordleeva, Sarika Jalan, Mikhail Ivanchenko, Oleg Kanakov, Valentina Kustikova, Ines P. Mariño, Iosif Meyerov, Ekkehard Ullner, Claudio Franceschi, and Alexey Zaikin. The human body as a super network: Digital methods to analyze the propagation of aging. *Frontiers in Aging Neuroscience*, 12, May 2020.
3. Bryce A. Mander, Joseph R. Winer, and Matthew P. Walker. Sleep and human aging. *Neuron*, 94(1):19–36, apr 2017.
4. Saranya Sundaram, Rachel L. Hughes, Eric Peterson, Eva M. Müller-Oehring, Helen M. Brontë-Stewart, Kathleen L. Poston, Afik Faerman, Chloe Bhowmick, and Tilman Schulte. Establishing a framework for neuropathological correlates and glymphatic system functioning in Parkinson’s disease. *Neuroscience & Biobehavioral Reviews*, 103:305–315, aug 2019.
5. L. Xie, H. Kang, Q. Xu, M. J. Chen, Y. Liao, M. Thiyagarajan, J. O’Donnell, D. J. Christensen, C. Nicholson, J. J. Iliff, T. Takano, R. Deane, and M. Nedergaard. Sleep drives metabo-

- lite clearance from the adult brain. *Science*, 342:373–377, Oct 2013.
6. Nadia Aalling Jessen, Anne Sofie Finmann Munk, Iben Lundgaard, and Maiken Nedergaard. The glymphatic system: A beginner’s guide. *Neurochemical Research*, 40(12):2583–2599, may 2015.
7. J. J. Iliff, M. Wang, Y. Liao, B. A. Plogg, W. Peng, G. A. Gundersen, H. Benveniste, G. E. Vates, R. Deane, S. A. Goldman, E. A. Nagelhus, and M. Nedergaard. A paravascular pathway facilitates CSF flow through the brain parenchyma and the clearance of interstitial solutes, including amyloid  $\beta$ . *Science Translational Medicine*, 4(147):147ra111–147ra111, aug 2012.
8. J. J. Iliff and M. Nedergaard. Is there a cerebral lymphatic system? *Stroke*, 44(6, Supplement 1):S93–S95, may 2013.
9. Benjamin T. Kress, Jeffrey J. Iliff, Maosheng Xia, Minghuan Wang, Helen S. Wei, Douglas Zeppenfeld, Lulu Xie, Hongyi Kang, Qiwu Xu, Jason A. Liew, Benjamin A. Plog, Fengfei Ding, Rashid Deane, and Maiken Nedergaard. Impairment of paravascular clearance pathways in the aging brain. *Annals of Neurology*, 76(6):845–861, sep 2014.
10. I.C.M. Verheggen, M.P.J. Van Boxtel, F.R.J. Verhey, J.F.A. Jansen, and W.H. Backes. Interaction between blood-brain barrier and glymphatic system in solute clearance. *Neuroscience & Biobehavioral Reviews*, 90:26–33, jul 2018.
11. Jenna M. Tarasoff-Conway, Roxana O. Carare, Ricardo S. Osorio, Lidia Glodzik, Tracy Butler, Els Fieremans, Leon Axel, Henry Rusinek, Charles Nicholson, Berislav V. Zlokovic, Blas Frangione, Kaj Blennow, Joël Ménard, Henrik Zetterberg, Thomas Wisniewski, and Mony J. de Leon. Clearance systems in the brain — implications for Alzheimer disease. *Nature Reviews Neurology*, 11(8):457–470, jul 2015.
12. N. Joan Abbott, Adjanie A.K. Patabendige, Diana E.M. Dolman, Siti R. Yusof, and David J. Begley. Structure and function of the blood–brain barrier. *Neurobiology of Disease*, 37(1):13–25, jan 2010.
13. K.-J. Yin, J. R. Cirrito, P. Yan, X. Hu, Q. Xiao, X. Pan, R. Bateman, H. Song, F.-F. Hsu, J. Turk, J. Xu, C. Y. Hsu, J. C. Mills, D. M. Holtzman, and J.-M. Lee. Matrix metalloproteinases expressed by astrocytes mediate extracellular amyloid-beta peptide catabolism. *Journal of Neuroscience*, 26(43):10939–10948, oct 2006.
14. Donna M Wilcock, Sanjay K Munireddy, Arnon Rosenthal, Kenneth E Ugen, Marcia N Gordon, and Dave Morgan. Microglial activation facilitates  $A\beta$  plaque removal following intracranial

- anti-A $\beta$  antibody administration. *Neurobiology of Disease*, 15(1):11–20, feb 2004.
15. C. A. Hawkes and J. McLaurin. Selective targeting of perivascular macrophages for clearance of  $\beta$ -amyloid in cerebral amyloid angiopathy. *Proceedings of the National Academy of Sciences*, 106(4):1261–1266, jan 2009.
  16. Christopher D. Morrone, Mingzhe Liu, Sandra E. Black, and JoAnne McLaurin. Interaction between therapeutic interventions for Alzheimer's disease and physiological A $\beta$  clearance mechanisms. *Frontiers in Aging Neuroscience*, 7, may 2015.
  17. Michael W Salter and Beth Stevens. Microglia emerge as central players in brain disease. *Nature Medicine*, 23(9):1018–1027, sep 2017.
  18. Tuan Leng Tay, Julie C. Savage, Chin Wai Hui, Kanchan Bisht, and Marie-Ève Tremblay. Microglia across the lifespan: from origin to function in brain development, plasticity and cognition. *The Journal of Physiology*, 595(6):1929–1945, may 2016.
  19. Katrin Kierdorf and Marco Prinz. Microglia in steady state. *Journal of Clinical Investigation*, 127(9):3201–3209, jul 2017.
  20. Anzela Niraula, John F Sheridan, and Jonathan P Godbout. Microglia priming with aging and stress. *Neuropsychopharmacology*, 42(1):318–333, sep 2016.
  21. Rodney M. Ritzel, Anita R. Patel, Sarah Pan, Joshua Crapser, Matt Hammond, Evan Jellison, and Louise D. McCullough. Age- and location-related changes in microglial function. *Neurobiology of Aging*, 36(6):2153–2163, jun 2015.
  22. Laura E. Clarke, Shane A. Liddelow, Chandrani Chakraborty, Alexandra E. Münch, Myriam Heiman, and Ben A. Barres. Normal aging induces A1-like astrocyte reactivity. *Proceedings of the National Academy of Sciences*, 115(8):E1896–E1905, feb 2018.
  23. Janet M. Mullington, Norah S. Simpson, Hans K. Meier-Ewert, and Monika Haack. Sleep loss and inflammation. *Best Practice & Research Clinical Endocrinology & Metabolism*, 24(5):775–784, oct 2010.
  24. Gabriela Hurtado-Alvarado, Lenin Pavón, Stephanie Ariadne Castillo-García, María Eugenia Hernández, Emilio Domínguez-Salazar, Javier Velázquez-Moctezuma, and Beatriz Gómez-González. Sleep loss as a factor to induce cellular and molecular inflammatory variations. *Clinical and Developmental Immunology*, 2013:1–14, 2013.
  25. Michael R. Irwin, Richard Olmstead, and Judith E. Carroll. Sleep disturbance, sleep duration, and inflammation: A systematic review and meta-analysis of cohort studies and experimental sleep deprivation. *Biological Psychiatry*, 80(1):40–52, jul 2016.
  26. Michele Bellesi, Luisa de Vivo, Mattia Chini, Francesca Gilli, Giulio Tononi, and Chiara Cirelli. Sleep loss promotes astrocytic phagocytosis and microglial activation in mouse cerebral cortex. *The Journal of Neuroscience*, 37(21):5263–5273, may 2017.
  27. V. Hugh Perry and Clive Holmes. Microglial priming in neurodegenerative disease. *Nature Reviews Neurology*, 10(4):217–224, mar 2014.
  28. E. L. Boespflug and J. J. Iliff. The emerging relationship between interstitial fluid-cerebrospinal fluid exchange, amyloid- $\beta$ , and sleep. *Biological psychiatry*, 83:328–336, Feb 2018.
  29. Judith E. Carroll, Steven W. Cole, Teresa E. Seeman, Elizabeth C. Breen, Tuff Witarama, Jesusa M.G. Arevalo, Jeffrey Ma, and Michael R. Irwin. Partial sleep deprivation activates the DNA damage response (DDR) and the senescence-associated secretory phenotype (SASP) in aged adult humans. *Brain, Behavior, and Immunity*, 51:223–229, January 2016.
  30. Rodney M. Ritzel, Sarah J. Doran, Ethan P. Glaser, Victoria E. Meadows, Alan I. Faden, Bogdan A. Stoica, and David J. Loane. Old age increases microglial senescence, exacerbates secondary neuroinflammation, and worsens neurological outcomes after acute traumatic brain injury in mice. *Neurobiology of Aging*, 77:194–206, may 2019.
  31. D. J. Baker and R. C. Petersen. Cellular senescence in brain aging and neurodegenerative diseases: evidence and perspectives. *The Journal of clinical investigation*, 128:1208–1216, Apr 2018.
  32. Antero Salminen, Johanna Ojala, Kai Kaarniranta, Annakaisa Haapasalo, Mikko Hiltunen, and Hilikka Soininen. Astrocytes in the aging brain express characteristics of senescence-associated secretory phenotype. *European Journal of Neuroscience*, 34(1):3–11, jun 2011.
  33. Judith Campisi. Aging, cellular senescence, and cancer. *Annual Review of Physiology*, 75(1):685–705, feb 2013.
  34. Natalie C Chen, Andrea T Partridge, Ferit Tuzer, Justin Cohen, Timothy Nacarelli, Sonia Navas-Martín, Christian Sell, Claudio Torres, and Julio Martín-García. Induction of a senescence-like phenotype in cultured human fetal microglia during HIV-1 infection. *The Journals of Gerontology: Series A*, 73(9):1187–1196, feb 2018.
  35. Glyn Nelson, James Wordsworth, Chunfang Wang, Diana Jurk, Conor Lawless, Carmen Martin-Ruiz, and Thomas von Zglinicki. A senescent cell bystander effect: senescence-induced senescence. *Aging Cell*, 11(2):345–349, feb 2012.
  36. Francesco Prattichizzo, Massimiliano Bonafè, Fabiola Olivieri, and Claudio Franceschi. Senescence associated macrophages and “macroph-aging”: are they pieces of the same puzzle? *Aging*, 8(12):3159–3160, dec 2016.
  37. C. Franceschi and J. Campisi. Chronic inflammation (inflammaging) and its potential contribution to age-associated diseases. *The Journals of Gerontology Series A: Biological Sciences and Medical Sciences*, 69(Suppl 1):S4–S9, may 2014.
  38. Claudio Franceschi, Paolo Garagnani, Paolo Parini, Cristina Giuliani, and Aurelia Santoro. Inflammaging: a new immune-metabolic viewpoint for age-related diseases. *Nature Reviews Endocrinology*, 14(10):576–590, jul 2018.
  39. Claudio Franceschi, Alexey Zaikin, Susanna Gordleeva, Mikhail Ivanchenko, Francesca Bonifazi, Gianluca Storci, and Massimiliano Bonafè. Inflammaging 2018: An update and a model. *Seminars in Immunology*, 40:1–5, December 2018.
  40. Claudio Franceschi, Paolo Garagnani, Giovanni Vitale, Miriam Capri, and Stefano Salvioli. Inflammaging and ‘garb-aging’. *Trends in Endocrinology & Metabolism*, 28(3):199–212, mar 2017.
  41. Hartmut Wekerle. Brain inflammatory cascade controlled by gut-derived molecules. *Nature*, 557(7707):642–643, may 2018.
  42. Benjamin Gompertz. XXIV. On the nature of the function expressive of the law of human mortality, and on a new mode of determining the value of life contingencies. In a letter to Francis Baily, Esq. F. R. S. &c. *Philosophical Transactions of the Royal Society of London*, 115:513–583, dec 1825.
  43. K. S. Brown, B. Math, and W. F. Forbes. A mathematical model of aging processes. II. *Journal of Gerontology*, 29(4):401–409, jul 1974.
  44. Avikar Periwal. Cellular senescence in the Penna model of aging. *Physical Review E*, 88(5), nov 2013.
  45. Nazareno G. F. de Medeiros and Roberto N. Onody. Heumann-Hötzel model for aging revisited. *Phys. Rev. E*, 64:041915, Sep 2001.
  46. Swadhin Taneja, Arnold B. Mitnitski, Kenneth Rockwood, and Andrew D. Rutenberg. Dynamical network model for age-related health deficits and mortality. *Physical Review E*, 93(2), feb 2016.
  47. Spencer G. Farrell, Arnold B. Mitnitski, Olga Theou, Kenneth Rockwood, and Andrew D. Rutenberg. Probing the network structure of health deficits in human aging. *Phys. Rev. E*, 98:032302, Sep 2018.
  48. Spencer G. Farrell, Arnold B. Mitnitski, Kenneth Rockwood, and Andrew D. Rutenberg. Network model of human aging: Frailty limits and information measures. *Phys. Rev. E*, 94:052409, Nov 2016.

49. August Weismann. The duration of life. In E. B. Poulton, S. Schönland, and A. E. Shipley, editors, *Essays upon heredity and kindred biological problems. Authorised translation*. Clarendon Press, Oxford, 1889.
50. R. Pearl. *The rate of living: Being an account of some experimental studies on the biology of life duration*. Knopf, New York, 1928.
51. RS Sohal. The rate of living theory: a contemporary interpretation. In K. G. Collatz and R. S. Sohal, editors, *Insect aging*, pages 23–44. Springer, 1986.
52. Peter Brian Medawar. *An unsolved problem of biology: an inaugural lecture delivered at University College, London, 6 December 1951*. H.K. Lewis & Co. for U.C.L., London, 1952. Reprinted in [53].
53. Peter Brian Medawar. An unsolved problem of biology. In *The uniqueness of the individual*, chapter 2, pages 44–70. Basic Books, New York, 1957.
54. Denham Harman. Extending functional life span. *Experimental Gerontology*, 33(1-2):95–112, jan 1998.
55. N. M. Emanuel. Free radicals and the action of inhibitors of radical processes under pathological states and ageing in living organisms and in man. *Quarterly Reviews of Biophysics*, 9(2):283–308, 1976.
56. R. M. Nesse and G. C. Williams. Evolution by natural selection. In *Evolution and Healing: New Science of Darwinian Medicine*, chapter 4, pages 13–25. Weidenfeld & Nicolson, London, 1995.
57. J. M. Clarke and J. M. Smith. Two phases of ageing in drosophila subobscura. *Journal of Experimental Biology*, 38(3):679–684, 1961.
58. J. Maynard Smith. Temperature and the rate of ageing in poikilotherms. *Nature*, 199(4891):400–402, 1963.
59. T. B. L. Kirkwood. Evolution of ageing. *Nature*, 270(5635):301–304, 1977.
60. Georgi P. Gladyshev. Thermodynamic theory of biological evolution and aging. Experimental confirmation of theory. *Entropy*, 1(4):55–68, 1999.
61. A. M. Olovnikov. The redosome hypothesis of aging and the control of biological time during individual development. *Biochemistry (Moscow)*, 68:2–33, 2003.
62. Simon Holbek, Kristian Moss Bendtsen, and Jeppe Juul. Moderate stem-cell telomere shortening rate postpones cancer onset in a stochastic model. *Phys. Rev. E*, 88:042706, Oct 2013.
63. Mark T. Mc Auley and Kathleen M. Mooney. Computationally modeling lipid metabolism and aging: A mini-review. *Computational and Structural Biotechnology Journal*, 13:38–46, 2015.
64. Mark T. Mc Auley, Alvaro Martinez Guimera, David Hodgson, Neil McDonald, Kathleen M. Mooney, Amy E. Morgan, and Carole J. Proctor. Modelling the molecular mechanisms of aging. *Bioscience Reports*, 37(1), feb 2017.
65. Jan Vijg and Yousin Suh. Genome instability and aging. *Annual Review of Physiology*, 75(1):645–668, feb 2013.
66. Ovide Arino, Marek Kimmel, and Glenn F. Webb. Mathematical modeling of the loss of telomere sequences. *Journal of Theoretical Biology*, 177(1):45–57, nov 1995.
67. Peter Olofsson and Marek Kimmel. Stochastic models of telomere shortening. *Mathematical Biosciences*, 158(1):75–92, apr 1999.
68. Zheng Tan. Telomere shortening and the population size-dependency of life span of human cell culture: further implication for two proliferation-restricting telomeres. *Experimental Gerontology*, 34(7):831–842, nov 1999.
69. Johnathan Labbadia and Richard I Morimoto. The biology of proteostasis in aging and disease. *Annual Review of Biochemistry*, 84(1):435–464, jun 2015.
70. Jianguyng Zou, Yongle Guo, Toumy Guettouche, David F Smith, and Richard Voellmy. Repression of heat shock transcription factor HSF1 activation by HSP90 (HSP90 complex) that forms a stress-sensitive complex with HSF1. *Cell*, 94(4):471–480, aug 1998.
71. Juliane Liepe, Hermann-Georg Holzthütter, Elena Bellavista, Peter M Kloetzel, Michael PH Stumpf, and Michele Mishto. Quantitative time-resolved analysis reveals intricate, differential regulation of standard- and immuno-proteasomes. *eLife*, 4, sep 2015.
72. Carole J Proctor, Maria Tsirigotis, and Douglas A Gray. An in silico model of the ubiquitin-proteasome system that incorporates normal homeostasis and age-related decline. *BMC Systems Biology*, 1(1), mar 2007.
73. I Tavassoly, J Parmar, AN Shajahan-Haq, R Clarke, WT Baumann, and JJ Tyson. Dynamic modeling of the interaction between autophagy and apoptosis in mammalian cells. *CPT: Pharmacometrics & Systems Pharmacology*, 4(4):263–272, apr 2015.
74. M. Schulzer, C. S. Lee, E. K. Mak, F. J. G. Vingerhoets, and D. B. Calne. A mathematical model of pathogenesis in idiopathic parkinsonism. *Brain*, 117(3):509–516, 1994.
75. A. Raichur, S. Vali, and F. Gorin. Dynamic modeling of alpha-synuclein aggregation for the sporadic and genetic forms of Parkinson’s disease. *Neuroscience*, 142(3):859–870, oct 2006.
76. Carole J. Proctor, Paul J. Tangeman, and Helen C. Ardley. Modelling the role of UCH-L1 on protein aggregation in age-related neurodegeneration. *PLoS ONE*, 5(10):e13175, oct 2010.
77. M. Cloutier and P. Wellstead. Dynamic modelling of protein and oxidative metabolisms simulates the pathogenesis of Parkinson’s disease. *IET Systems Biology*, 6(3):65, 2012.
78. Carole J Proctor, Ilse Pienaar, Joanna L Elson, and Thomas BL Kirkwood. Aggregation, impaired degradation and immunization targeting of amyloid-beta dimers in Alzheimer’s disease: a stochastic modelling approach. *Molecular Neurodegeneration*, 7(1):32, 2012.
79. Denham Harman. The biologic clock: The mitochondria? *Journal of the American Geriatrics Society*, 20(4):145–147, apr 1972.
80. A. Kowald and T. B. L. Kirkwood. Evolution of the mitochondrial fusion-fission cycle and its role in aging. *Proceedings of the National Academy of Sciences*, 108(25):10237–10242, jun 2011.
81. P. Dalle Pezze, A. G. Sonntag, A. Thien, M. T. Prentzell, M. Godel, S. Fischer, E. Neumann-Haefelin, T. B. Huber, R. Baumeister, D. P. Shanley, and K. Thedieck. A dynamic network model of mTOR signaling reveals TSC-independent mTORC2 regulation. *Science Signaling*, 5(217):ra25–ra25, mar 2012.
82. Annika G. Sonntag, Piero Dalle Pezze, Daryl P. Shanley, and Kathrin Thedieck. A modelling-experimental approach reveals insulin receptor substrate (IRS)-dependent regulation of adenosine monophosphate-dependent kinase (AMPK) by insulin. *FEBS Journal*, 279(18):3314–3328, may 2012.
83. Piero Dalle Pezze, Glyn Nelson, Elsje G. Otten, Viktor I. Korolchuk, Thomas B. L. Kirkwood, Thomas von Zglinicki, and Daryl P. Shanley. Dynamic modelling of pathways to cellular senescence reveals strategies for targeted interventions. *PLoS Computational Biology*, 10(8):e1003728, aug 2014.
84. A. Oeckinghaus and S. Ghosh. The NF- $\kappa$ B family of transcription factors and its regulation. *Cold Spring Harbor Perspectives in Biology*, 1(4):a000034–a000034, sep 2009.
85. Johanna Napetschnig and Hao Wu. Molecular basis of NF- $\kappa$ B signaling. *Annual Review of Biophysics*, 42(1):443–468, may 2013.
86. Soumen Basak, Marcelo Behar, and Alexander Hoffmann. Lessons from mathematically modeling the NF- $\kappa$ B pathway. *Immunological Reviews*, 246(1):221–238, mar 2012.
87. Richard Williams, Jon Timmis, and Eva Qvarnstrom. Computational models of the NF- $\kappa$ B signalling pathway. *Computation*, 2(4):131–158, sep 2014.
88. Jeremy D. Scheff, Steve E. Calvano, Stephen F. Lowry, and Ioannis P. Androulakis. Modeling the influence of circadian rhythms on the acute inflammatory response. *Journal of Theoretical Biology*, 264(3):1068–1076, jun 2010.



89. Andrew P. McGovern, Benjamin E. Powell, and Timothy J.T. Chevassut. A dynamic multi-compartmental model of DNA methylation with demonstrable predictive value in hematological malignancies. *Journal of Theoretical Biology*, 310:14–20, oct 2012.
90. Jens Przybilla, Thimo Rohlf, Markus Loeffler, and Joerg Galle. Understanding epigenetic changes in aging stem cells — a computational model approach. *Aging Cell*, 13(2):320–328, jan 2014.
91. T. Smith-Vikos and F. J. Slack. MicroRNAs and their roles in aging. *Journal of Cell Science*, 125(1):7–17, jan 2012.
92. Xin Lai, Olaf Wolkenhauer, and Julio Vera. Understanding microRNA-mediated gene regulatory networks through mathematical modelling. *Nucleic Acids Research*, 44(13):6019–6035, jun 2016.
93. Carlos López-Otín, Maria A. Blasco, Linda Partridge, Manuel Serrano, and Guido Kroemer. The hallmarks of aging. *Cell*, 153(6):1194–1217, jun 2013.
94. Vanja Pekovic and Christopher J. Hutchison. Adult stem cell maintenance and tissue regeneration in the ageing context: the role for A-type lamins as intrinsic modulators of ageing in adult stem cells and their niches. *Journal of Anatomy*, 213(1):5–25, jul 2008.
95. Dominik Duscher, Robert C. Rennert, Michael Januszzyk, Ersilia Anghel, Zeshaan N. Maan, Alexander J. Whittam, Marcelina G. Perez, Revanth Kosaraju, Michael S. Hu, Graham G. Walmsley, David Atashroo, Sacha Khong, Atul J. Butte, and Geoffrey C. Gurtner. Aging disrupts cell subpopulation dynamics and diminishes the function of mesenchymal stem cells. *Scientific Reports*, 4(1), nov 2014.
96. Christina Rose Kyrtos and John S. Baras. Modeling the role of the glymphatic pathway and cerebral blood vessel properties in Alzheimer's disease pathogenesis. *PLOS ONE*, 10(10):e0139574, oct 2015.
97. Jean-Christophe Leloup and Albert Goldbeter. Modeling the circadian clock: From molecular mechanism to physiological disorders. *BioEssays*, 30(6):590–600, 2008.
98. Atilla Altinok, Francis Lévi, and Albert Goldbeter. A cell cycle automaton model for probing circadian patterns of anticancer drug delivery. *Advanced Drug Delivery Reviews*, 59(9-10):1036–1053, aug 2007.
99. Michael R. Irwin. Sleep and inflammation: partners in sickness and in health. *Nature Reviews Immunology*, 19(11):702–715, jul 2019.
100. Luciana Besedovsky, Tanja Lange, and Monika Haack. The sleep-immune crosstalk in health and disease. *Physiological Reviews*, 99(3):1325–1380, jul 2019.
101. Urs Albrecht and Jürgen A. Ripperger. Circadian clocks and sleep: Impact of rhythmic metabolism and waste clearance on the brain. *Trends in Neurosciences*, 41(10):677–688, oct 2018.
102. Martin Kaag Rasmussen, Humberto Mestre, and Maiken Nedergaard. The glymphatic pathway in neurological disorders. *The Lancet Neurology*, 17(11):1016–1024, nov 2018.
103. Yuuki Obata, Álvaro Castaño, Stefan Boeing, Ana Carina Bon-Frauches, Candice Fung, Todd Fallesen, Mercedes Gomez de Agüero, Bahtiyar Yilmaz, Rita Lopes, Almaz Huseynova, Stuart Horswell, Muralidhara Rao Maradana, Werend Boesmans, Pieter Vanden Berghe, Andrew J. Murray, Brigitta Stockinger, Andrew J. Macpherson, and Vassilis Pachnis. Neuronal programming by microbiota regulates intestinal physiology. *Nature*, 578(7794):284–289, feb 2020.
104. Claudio Franceschi, Rita Ostan, and Aurelia Santoro. Nutrition and inflammation: Are centenarians similar to individuals on calorie-restricted diets? *Annual Review of Nutrition*, 38(1):329–356, August 2018.
105. Sari Stenholm, Jenny Head, Mika Kivimäki, Linda L Magnusson Hanson, Jaana Pentti, Naja H Rod, Alice J Clark, Tuula Oksanen, Hugo Westerlund, and Jussi Vahtera. Sleep duration and sleep disturbances as predictors of healthy and chronic disease-free life expectancy between ages 50 and 75: A pooled analysis of three cohorts. *The Journals of Gerontology: Series A*, 74(2):204–210, February 2018.
106. Eleonora Tobaldini, Elisa M. Fiorelli, Monica Solbiati, Giorgio Costantino, Lino Nobili, and Nicola Montano. Short sleep duration and cardiometabolic risk: from pathophysiology to clinical evidence. *Nature Reviews Cardiology*, 16(4):213–224, November 2018.
107. Erin O. Wissler Gerdes, Yi Zhu, Tamar Tchkonina, and James L. Kirkland. Discovery, development, and future application of senolytics: theories and predictions. *The FEBS Journal*, 287(12):2418–2427, March 2020.
108. Sundeep Khosla, Joshua N. Farr, Tamara Tchkonina, and James L. Kirkland. The role of cellular senescence in ageing and endocrine disease. *Nature Reviews Endocrinology*, 16(5):263–275, March 2020.
109. Nicolas Musi, Joseph M. Valentine, Kathryn R. Sickora, Eric Baeuerle, Cody S. Thompson, Qiang Shen, and Miranda E. Orr. Tau protein aggregation is associated with cellular senescence in the brain. *Aging Cell*, 17(6):e12840, October 2018.
110. Peisu Zhang, Yuki Kishimoto, Ioannis Grammatikakis, Kamalvishnu Gottimukkala, Roy G. Cutler, Shiliang Zhang, Kotb Abdelmohsen, Vilhelm A. Bohr, Jyoti Misra Sen, Myriam Gorospe, and Mark P. Mattson. Senolytic therapy alleviates  $\alpha\beta$ -associated oligodendrocyte progenitor cell senescence and cognitive deficits in an alzheimer's disease model. *Nature Neuroscience*, 22(5):719–728, April 2019.
111. Shankar J. Chinta, Georgia Woods, Marco Demaria, Anand Rane, Ying Zou, Amanda McQuade, Subramanian Rajagopalan, Chandani Limbad, David T. Madden, Judith Campisi, and Julie K. Andersen. Cellular senescence is induced by the environmental neurotoxin paraquat and contributes to neuropathology linked to parkinson's disease. *Cell Reports*, 22(4):930–940, January 2018.
112. Tyler J. Bussian, Asef Aziz, Charlton F. Meyer, Barbara L. Swenson, Jan M. van Deursen, and Darren J. Baker. Clearance of senescent glial cells prevents tau-dependent pathology and cognitive decline. *Nature*, 562(7728):578–582, September 2018.
113. LaTonya J. Hickson, Larissa G.P. Langhi Prata, Shane A. Bobart, Tamara K. Evans, Nino Giordagze, Shahrukh K. Hashmi, Sandra M. Herrmann, Michael D. Jensen, Qingyi Jia, Kyra L. Jordan, Todd A. Kellogg, Sundeep Khosla, Daniel M. Koerber, Anthony B. Lagnado, Donna K. Lawson, Nathan K. LeBrasseur, Lilach O. Lerman, Kathleen M. McDonald, Travis J. McKenzie, João F. Passos, Robert J. Pignolo, Tamar Pirtskhalava, Ishran M. Saadiq, Kalli K. Schaefer, Stephen C. Textor, Stella G. Victorelli, Tammie L. Volkman, Ailing Xue, Mark A. Wentworth, Erin O. Wissler Gerdes, Yi Zhu, Tamara Tchkonina, and James L. Kirkland. Senolytics decrease senescent cells in humans: Preliminary report from a clinical trial of dasatinib plus quercetin in individuals with diabetic kidney disease. *EBioMedicine*, 47:446–456, September 2019.
114. Helene Benveniste, Xiaodan Liu, Sunil Koundal, Simon Sanggaard, Hedok Lee, and Joanna Wardlaw. The glymphatic system and waste clearance with brain aging: A review. *Gerontology*, 65(2):106–119, jul 2018.
115. Ming Xu, Elizabeth W. Bradley, Megan M. Weivoda, Soyun M. Hwang, Tamar Pirtskhalava, Teresa Decklever, Geoffry L. Curran, Mikolaj Ogrodnik, Diana Jurk, Kurt O. Johnson, Val Lowe, Tamar Tchkonina, Jennifer J. Westendorf, and James L. Kirkland. Transplanted senescent cells induce an osteoarthritis-like condition in mice. *The Journals of Gerontology Series A: Biological Sciences and Medical Sciences*, page glw154, aug 2016.
116. Brandon M. Hall, Vitaly Balan, Anatoli S. Gleiberman, Evguenia Strom, Peter Krasnov, Lauren P. Virtuoso, Elena Rydkina, Slavoljub Vujcic, Karina Balan, Ilya Gitlin, Katerina Leonova,

- Alexander Polinsky, Olga B. Chernova, and Andrei V. Gudkov. Aging of mice is associated with p16(Ink4a)- and  $\beta$ -galactosidase-positive macrophage accumulation that can be induced in young mice by senescent cells. *Aging*, 8(7):1294–1315, jul 2016.
117. Wai T. Wong. Microglial aging in the healthy CNS: phenotypes, drivers, and rejuvenation. *Frontiers in Cellular Neuroscience*, 7, 2013.